

R. WOJNAROWSKA\*, J. POLIT\*, #, D. BRODA\*\*, M. GONCHAR\*\*\*,\*\*\*\*, E. M. SHEREGII\*

**GOLD NANOPARTICLES LIKE A MATRIX FOR COVALENT IMMOBILIZATION OF CHOLESTEROL OXIDASE – APPLICATION FOR BIOSENSING**

**NANOCZĄSTKI ZŁOTA JAKO MATRYCA DO IMMOBILIZACJI OKSYDAZY CHOLESTEROLU – ZASTOSOWANIE W BIOSENSORACH**

Gold nanoparticles are emerging as promising agents for various areas of material science as well as nanotechnology, electronics and medicine. The interest in this material is provided due to its unique optical, electronic and molecular-recognition properties. This paper presents results of preparation, characterization and biofunctionalization of gold nanoparticles. Nanoparticles have been conjugated with the cholesterol oxidase enzyme in order to prepare the active element for biosensors. Cholesterol oxidase is one of the most important analytical enzyme, used for cholesterol assay in clinical diagnostics, and there is still a necessity in improvement of existing analytical techniques, including bio-nanotechnological approaches based on modern nanosystems. The prepared bio-nanosystem was characterized by the enzyme activity test. Obtained results showed a stable binding of the enzyme with nanoparticles and preserved the bioactivity approves which gives possibility to use the prepared bio-nanosystems for analytical purposes.

The Surface Plazmon Resonance and the Surface Enhanced Raman Scattering as specific for nanocarriers effects were observed what enable us to research the oscillation spectra of enzyme. These spectra were compared with ones obtained by IR-spectroscopy. The vibrational lines are attributed to chemical functional groups existing in enzyme, for example, amino acids, amide groups as well as flavin – adenine dinucleotide cholesterol oxidase prosthetic group. By this way the identified spectral lines can be used as a distinguishing mark of enzyme.

**Keywords:** gold nanoparticles; biofunctionalization; enzyme; FTIR; SERS

Nanocząstki złota zdają się być niezwykle obiecującym materiałem, który z powodzeniem może być wykorzystywany w różnych dziedzinach inżynierii materiałowej, nanotechnologii, elektroniki czy medycyny. Zainteresowanie tym materiałem wynika z posiadanych przez niego unikatowych właściwości optycznych, elektronicznych i identyfikacji na poziomie molekularnym. W artykule przedstawiono wyniki prowadzonych badań dotyczących przygotowania, charakterystyki i biofunkcjonalizacji nanocząstek złota. Celem wytwarzania iłączenia nanocząstek złota z enzymem oksydazą cholesterolową było opracowanie aktywnego biologicznego elementu biosensora. Oksydaza cholesterolowa jest jednym z najważniejszych enzymów analitycznych, stosowanych w diagnostyce klinicznej do oznaczenia stężenia cholesterolu. Istnieje potrzeba doskonalenia istniejących metod analitycznych, między innymi poprzez wykorzystanie nowoczesnych nanomateriałów. Przeprowadzono badania aktywności enzymu immobilizowanego, jak również dokonano charakterystyki danego bionanosystemu za pomocą wybranych metod optycznych. Na podstawie uzyskanych wyników można stwierdzić, że wiązanie enzymu z nanocząstekami jest stabilne, a aktywność biologiczna została zachowana, co pozwala na przygotowanie bio-nanosystemu do celów analitycznych. Zaobserwowano również wystąpienie dwóch efektów optycznych charakterystycznych w przypadku zastosowania odpowiednich nanonośników: Powierzchniowego Rezonansu Plazmonów oraz Powierzchniowo Wzmocnionego Rozproszenia Ramanowskiego. Uzyskane widma były porównywane z widmami w podczerwieni. Zaobserwowane linie przypisano do charakterystycznych grup funkcyjnych, aminokwasów, wiązań peptydowych, jak również dinukleotydu flawinoadeninowego czyli grupy prostetycznej oksydazy cholesterolowej. Zidentyfikowane linie mogą być wykorzystywane jako marker analityczny dla danego enzymu.

\* UNIVERSITY OF RZESZOW, CENTER FOR MICROELECTRONICS AND NANOTECHNOLOGY, 1 PIGONIA STR., 35-959 RZESZOW, POLAND

\*\* UNIVERSITY OF RZESZOW, DEPARTMENT OF BIOTECHNOLOGY, INSTITUTE OF APPLIED BIOTECHNOLOGY AND BASIC SCIENCES, 36 SOKOLOWSKA STR., 36-100 KOLBUSZOWA, POLAND

\*\*\* NATIONAL ACADEMY OF SCIENCES OF UKRAINE, INSTITUTE OF CELL BIOLOGY, 14/16 DRAHOMANOV STR., 79005 LVIV, UKRAINE

# Corresponding author: polijack@ur.edu.pl

## 1. Introduction

In the past few years, the researches on nanocarriers, that are biocompatible and useful for medical purposes, has increased very quickly. The biomolecules (enzymes or antibodies, for example) bounded with metal nanoparticles and oxide nanoparticles enable us to achieve an increased detection signal in different analytical methods [1,2]. Unique optical properties of noble metal nanoparticles (NPs), for example, the possibility of plasmon exciting (so called Surface Plasmon Resonance – SPR), can be useful in modern diagnostic methods for optical biosensors developed [3-5]. Surface Enhanced Raman Scattering (SERS) has emerged as a powerful analytical tool that extends the possibilities of vibrational spectroscopy [6-8], but they need a suitable matrix which allows the maximum amplification of the signal coming from tested biomolecules. The gold nanoparticles (AuNPs) of different size, shape and composited with various substrates seems to be the most effective for this aim. From other hand, binding of noble metal NPs with enzymes is a construction for sensitive electrochemical biosensors because unique electrical properties. The AuNPs have an excellent conductivity and they are suitable for acting as “electronic wires” to enhance the transfer of electrons (from biological element to electrode) generated during the chemical reactions catalyzed by enzymes [9]. Simultaneously, the bioactivity of the enzyme is improved as well as stability also: the enzyme conjugated with the AuNPs is more stable in various environmental conditions and it is more stable during the time in comparison with a free enzyme [10].

Among the enzymes of analytical interest the cholesterol oxidase (ChOX) is used for the determination of the serum cholesterol content in clinical diagnostics [11-12]. It is an important biomarker of coronary heart disease, arteriosclerosis, and lipid metabolism dysfunction [13]. The ChOX is the flavin adenine dinucleotide (FAD) dependent enzyme [14]. The FAD (non-proteinaceous prosthetic group) is deeply seated in a protein core and its presence causes the enzyme catalytic activity because it enables the oxidation of cholesterol) [11]. Thus, development of improved analytical methods, such as contemporary and sensitive biosensors as well as the immobilization and stabilization of the corresponding enzyme, is still ongoing [15].

In this work, results of preparation and biofunctionalization of the AuNPs are presented. The nanoparticles were characterized by microscopic and spectroscopic technique. The cholesterol oxidase enzyme (EC 1.1.3.6) is bounded to the surface of the AuNPs via 16-mercaptophexadecanoic acid (MHDA) organic linker. Observed vibrational lines are identified and attributed to corresponding chemical functional groups what is important for the biosensing application.

## 2. Experimental

### 2.1. Synthesis of gold nanoparticles and biofunctionalisation

The AuNPs are prepared by the Turkevich method [16]. For this aim, different ratios of chloroauric acid (1 mM) and reductant (34 mM trisodium citrate) are used as followed: a) 0.1 ml : 4.9 ml; b) 0.24 ml : 4.76 ml; c) 0.65 ml : 4.35 ml. The reagents were heated to 100°C and mixed. The boiling and stirring was continued for 15 minutes, until the color of the solution became red. The reaction mixtures were cooled, precipitated (by centrifugation at 24000g force) and washed twice with distilled water or toluene.

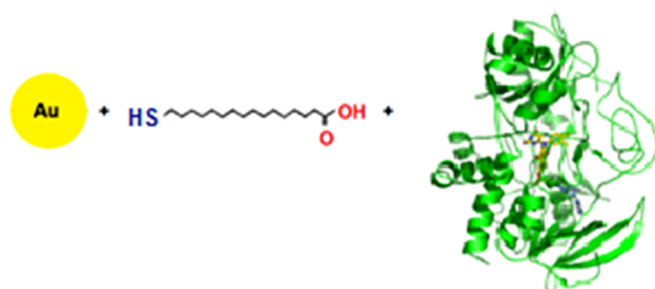


Fig. 1. Scheme of nanosystem consisting of AuNP, MHDA linker and cholesterol oxidase enzyme

In the next steps, the 16-mercaptophexadecanoic acid MHDA linker is bounded to the surface of nanoparticles [10] and ChOX enzyme is covalently immobilized with them as it shown in Fig. 1. The connection between the AuNPs and the MHDA linker is possible by presence of SH thiol group and Ag-S bond formation, while carboxyl group enables the protein binding. The AuNPs were incubated overnight with 5 mM MHDA solubilized in ethanol at temperature 4°C. The conjugate was rinsed with N,N-dimethylformamid (DMF) and N-cyclohexyl-N'-(2-morpholinoethyl)carbodiimidemetho-p-toluenesulfonate (CMC), 20 mM pentafluorophenyl-4-vinylbenzoate (PFP), 20 mM N,N-diisopropylethylamine (DIPEA) in DMF for 30 min at 25°C, under constant mixing. Then, prepared mixture of nanoparticles was suspended in 50 µl of 1 mg/ml ChOX solution in 50 mM phosphate buffer (pH 7.5) and incubated as above.

The ChOX produced by microorganisms – *Brevibacterium sp.* was purchased from the Roche Diagnostics company with the initial activity 15.3 U/mg. The enzyme concentration in the final colloidal solution was determined to be 0.5 mg/ml. The obtained samples were rinsed twice with phosphate buffer.

### 2.2. Measurements of the size, shape and efficiency of enzyme immobilization

The size, as well as the shape of the nanoparticles is measured after drying on the highest grade mica surface by atomic force microscope (AFM) Innova Bruker in tapping mode using silicon nitride cantilever.

The amount of protein in the supernatant is determined by a Bradford colorimetric method at 595 nm with using calibration curve of bovine serum albumin (BSA) as the protein standard.

### 2.3. The enzyme activity measurement

The activity of cholesterol oxidase is determined in reaction transformation of cholesterol to 4-cholesten-3-one and H<sub>2</sub>O<sub>2</sub>. The generated hydrogen peroxide was monitored in horseradish peroxidase-catalyzed reaction of oxidation of *o*-dianisidine by H<sub>2</sub>O<sub>2</sub>. The reaction mixture consisted 0.1% *o*-dianisidine, 0.025 % cholesterol, 0.15 mL horseradish peroxidase in phosphate buffer (50 mM, pH 7.0) and ChOX (free or bound with AuNPs). The colorimetric measurement is performed at 500 nm with using Tecan Infinite M200 spectrometer and calculated to enzyme activity.

### 2.4. Spectroscopic measurements

The AuNP+MHDA+ChOX bio-nanosystems described above are characterized by three optical methods: absorbance in the visible light (UV-VIS spectroscopy), transmission in the infrared region (FTIR) as well as the Raman spectroscopy. The

UV-VIS absorbance spectra of the aqueous colloid samples in commercial quartz cuvette were obtained using Evolution 300 UV-VIS spectrophotometer (Thermo Scientific) in the 400-900 nm range. The FTIR Spectroscopy measurements were performed by the Vertex 70 (Bruker) spectrometer with using the Attenuated Total Reflectance (ATR) technique involving diamond crystal. The measurements were performed in the region of middle infrared (400-4000 cm<sup>-1</sup>) using 32 scans provided spectral resolution of 2 cm<sup>-1</sup>.

The Raman spectra were obtained using the SmartRaman DXR (Thermo Scientific) spectrometer. The semiconductor laser of 14 mW power and 780 nm wavelength was used as a light source. Samples for the Raman spectroscopy were dried on small glass slides.

## 3. Results and discussion

### 3.1. Particles size and structure

The AFM images of the AuNPs and the AuNP+MHDA+ChOX complexes are shown in Fig. 2. As was noticed earlier [17], the size of the gold nanoparticles of different prepared samples is mainly dependent on concentration of the reducing agent. The smallest nanoparticles have size of about 42 nm and they are

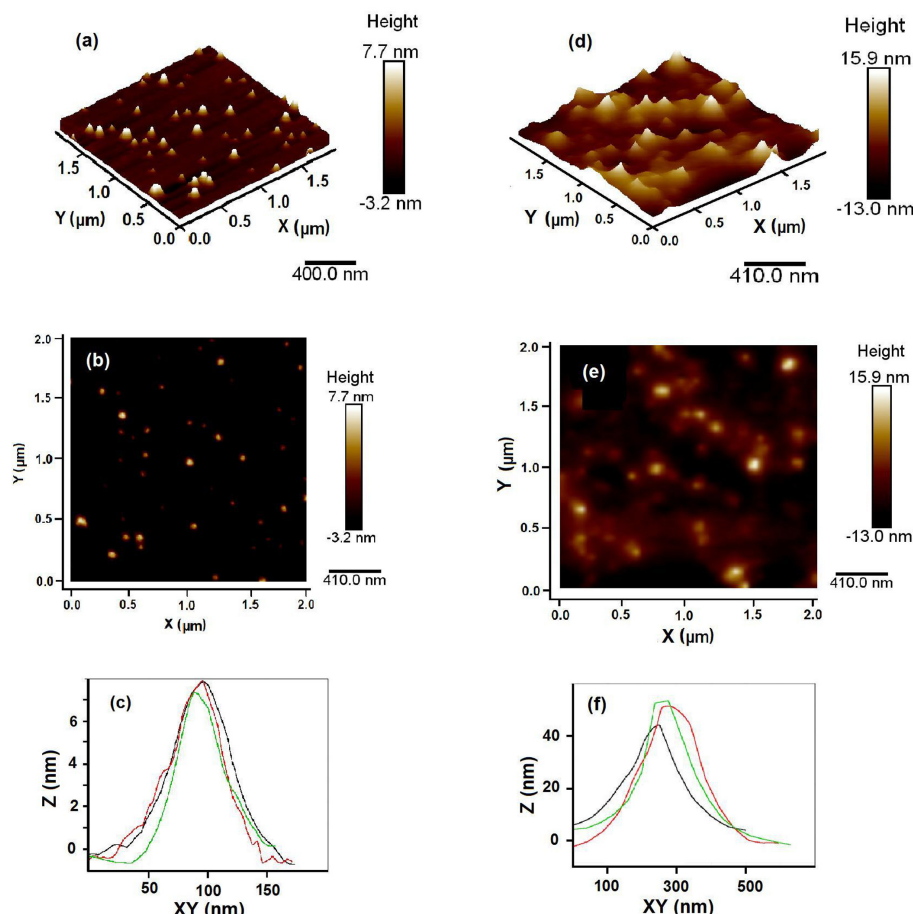


Fig. 2. AFM imaging of AuNPs: (a) 3D image; (b) 2D topography; (c) height profile; and AuNP+MHDA+ChOX complexes: (d) 3D image; (b) 2D topography; (c) height profile

prepared with the highest concentration of the sodium citrate as a reductant. Other samples have the sizes adequately equal to 55 nm and 80 nm. The AuNPs have mainly spherical shape, as it is shown in Fig. 2b.

In Fig. 2d-f there are presented the AFM images of gold nanoparticles conjugated with the enzyme. In all cases, the nanoparticles after conjugation with enzyme are in more aggregated form, than initial nanoparticles: the sizes are increased at about 80% and became more differentiated ones. Moreover, the shape of the particles is changed also - from spherical to more irregular.

### 3.2. Binding efficiency and enzyme activity in the AuNP+MHDA+ChOX bio-nanosystem

Free enzyme concentration was determined by measuring the protein content in the supernatant. It was found that almost all of the used enzyme was binding to the surface of nanoparticles. The efficiency of binding was noticed between 94 and 100%. These means that less than 6% of used enzyme is located in the supernatant after conjugation. The enzyme concentration in the final colloidal solution was determined to be 0.5 mg/ml. The binding of the ChOX to the AuNPs by the MHDA linker was confirmed also by spectroscopic method (see subchapter 3.4). The activity of the cholesterol oxidase enzyme in AuNP+MHDA+ChOX complex was confirmed by biochemical experiment – an activity ratio of 2,56 U/mg was determined. These value is less than output level, but is one still satisfactory. Negligible part only of enzyme molecules becomes inactive during the sample preparation process, furthermore, the binding between enzyme and nanoparticles is stable after rinsing.

### 3.3. SPR effect

In Fig. 3 are shown the absorbance spectra recorded by the UV-VIS Evolution 300 spectrometer for the colloidal solutions of pure AuNPs as well as for the AuNP+MHDA+ChOX com-

plexes. The absorption band for pure AuNPs is located at about 527 nm. These position is changed in the framework of  $\pm 4$  nm, depending on the size of the nanoparticles. The absorption band for the AuNP+MHDA+ChOX complex is shifted of 67 nm towards longer wavelengths in comparison with pure AuNPs and is located at 594 nm. This change of the plasmon frequency value is caused by transferring of part of electrons from the AuNP to the ligand what means decreasing of the electron concentration in the AuNPs matrix and decreasing of the Plasmon frequency shift the resonance band towards longer wavelength [18].

### 3.4. Infrared oscillation spectra

Chemical interactions between cholesterol oxidase, linker and nanoparticles as well as binding effectivity were studied by FTIR technique. Measurements were performed for pure AuNPs, AuNP+MHDA, free MHDA, and AuNP+MHDA+ChOX complex. The spectra obtained for the three steps of the sample preparation are collected in Fig. 4. The AuNPs spectrum contains the lines assigned to O-H, C-H, C = O chemical bonds derived from sodium citrate residues. The AuNP+MHDA spectrum is richer in the lines attributed to C-H bonds (at  $2914\text{ cm}^{-1}$ ,  $2848\text{ cm}^{-1}$ ,  $1472\text{ cm}^{-1}$ ,  $1407\text{ cm}^{-1}$ ) as well as the bands assigned to the carboxyl group (at  $1694\text{ cm}^{-1}$  associated with C = O, at  $3280\text{ cm}^{-1}$  – with O-H, at  $1428\text{ cm}^{-1}$  – with C-O bonds) [19-21]. The lines at  $714\text{ cm}^{-1}$  and  $684\text{ cm}^{-1}$  represent the S-C stretching vibrations [19]. The IR spectra confirms successful conjugation of the AuNPs with the MHDA linker. The S-H line at around  $2550\text{ cm}^{-1}$  was noticed in the spectrum of pure MHDA, but it is absent in the AuNP+MHDA spectrum, at indicates appearance of the Au-S bond [22].

Whereas, the AuNP+MHDA+ChOX spectrum in the  $1300\text{ cm}^{-1}$  to  $1700\text{ cm}^{-1}$  region possess a typical spectral lines corresponding to the proteins: the amide I, amide II and amide III bands [23]. That suggests effective binding of the enzyme with AuNPs by MHDA in the tested samples. The amide I band is observed at  $1642\text{ cm}^{-1}$  and corresponds mainly to the stretching vibration of the peptide carbonyl group (C = O), and to the C-N stretching vibrations also. The line at  $1540\text{ cm}^{-1}$  corresponds to the amide II band (mainly N-H bending and C-N stretching vibrations), and the amide III line at  $1256\text{ cm}^{-1}$  can be assigned also to the C-N, N-H and C-O stretching vibrations [24,25]. Moreover, the region from  $2800\text{ cm}^{-1}$  to  $3600\text{ cm}^{-1}$  is also interesting: observed lines can be assigned to the C-H, N-H and O-H stretching vibrations. The  $500$ - $1100\text{ cm}^{-1}$  region is called as the fingerprint region and is associated with the construction of the molecule's skeleton [19,26]. Moreover, in this region we observe the lines which should be assigned to the enzyme prosthetic group – the P-O bonds vibrations at  $986\text{ cm}^{-1}$  belonging to the flavin adenine dinucleotide (FAD) [19]. The position of observed lines and their interpretation is given in Table 1.

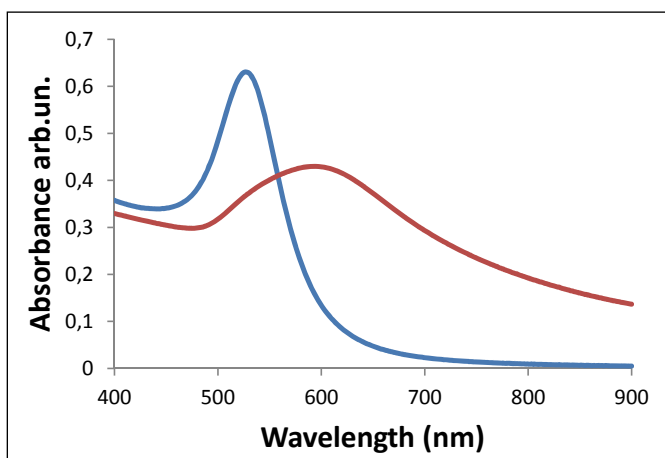


Fig. 3. SPR band of pure gold nanoparticles (blue curve) and nanoparticles conjugated with cholesterol oxidase (red curve)

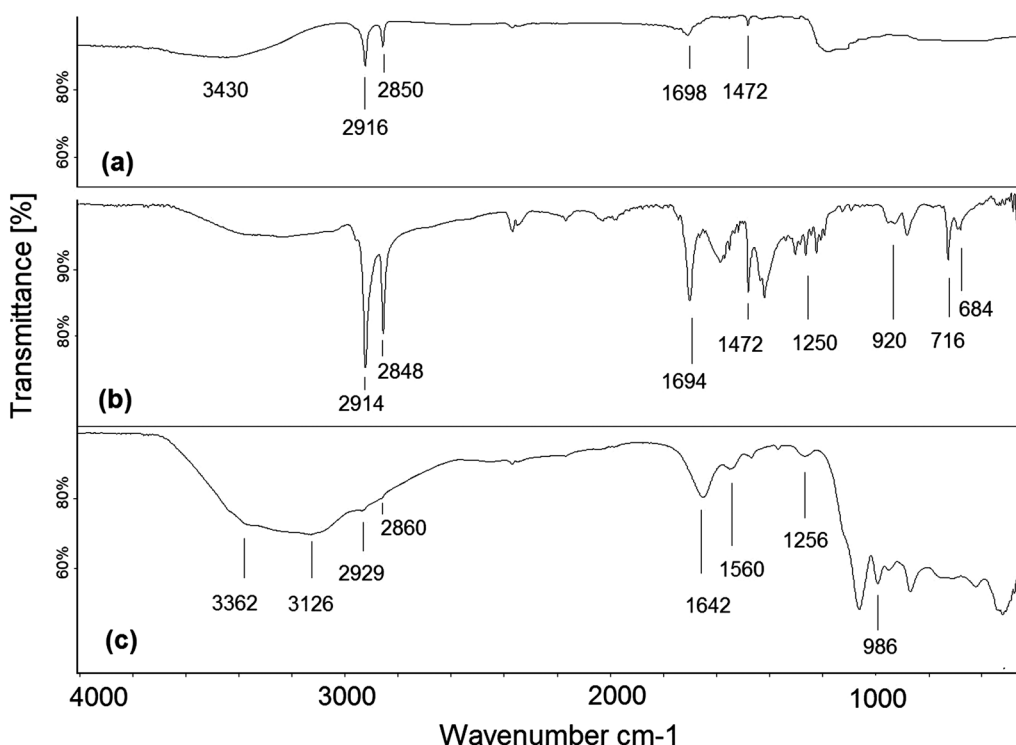


Fig. 4. FTIR spectra of the (a) AuNPs, (b) AuNP+MHDA, (c) AuNP+ MHDA+ChOX

TABLE 1

Identification of the lines observed in the FTIR spectra (Fig. 4)

	Position of line or group of lines ( $\text{cm}^{-1}$ )	Sample	Identification	Reference
1	3430/3280/3362	AuNP/AuNP+MHDA/AuNP+MHDA+ChOX	O-H stretch	19,20,21
2	3126	AuNP+MHDA+ChOX	N-H stretch	19,26
3	2916/2914/2929, 2850/2848/2860	AuNP/AuNP+MHDA/ AuNP+MHDA+ChOX	C-H stretch (asymmetric and symmetric)	19,20,21
4	1698/1694	AuNP/AuNP+MHDA	C = O	19,20,21
5	1642	AuNP+MHDA+ChOX	Amide I	23,24
6	1560	AuNP+MHDA+ChOX	Amide II	23,24
7	1472	AuNP/AuNP+MHDA	C-H bend	19,20,21
8	1428	AuNP+MHDA	C-O	19,20,21
9	1407	AuNP+MHDA	C-H bend	19,20,21
10	1256	AuNP+MHDA+ChOX	Amide III	23,24
11	986	AuNP+MHDA+ChOX	P-O (from FAD)	19
12	~920	AuNP+MHDA/ AuNP+MHDA+ChOX	C-C	19
13	716,684	AuNP+MHDA	C-S	19

### 3.5. SERS effect

It is well-known that the Raman backscattering experiment is complementary to the IR-transmission experiment. The oscillation lines in the Raman experiment are observed directly and immediately what could be used for biosensing, especially when we can obtain SERS effect, which allows to significantly improve the sensitivity of system.

In Fig. 4 are shown the Raman backscattering spectra for the AuNPs matrix, AuNP+MHDA and AuNP+MHDA+ChOX construct. The most interesting for the AuNPs is band at about

1250  $\text{cm}^{-1}$  assigned to the vibrations of Au plasmons [27]. The majority of AuNP+MHDA lines corresponding to C-H bond are observed at about 2900  $\text{cm}^{-1}$  and in the region from 700  $\text{cm}^{-1}$  to 1500  $\text{cm}^{-1}$ . In the same region we can find lines assigned to C-C and C-O bond as well [27,28]. The (c) curve in Fig. 4 is the Raman spectrum of cholesterol oxidase immobilized on the nanoparticles' surface with 80 nm size of the AuNPs. The most intense line observed at 1530  $\text{cm}^{-1}$  is assigned to the chemical bond characteristic for proteins: N-H, C-N and N-C-O bond vibrations [29]. Other bands characteristic for proteins [30] are observed at 1610  $\text{cm}^{-1}$  and around 1220  $\text{cm}^{-1}$ , they are assigned

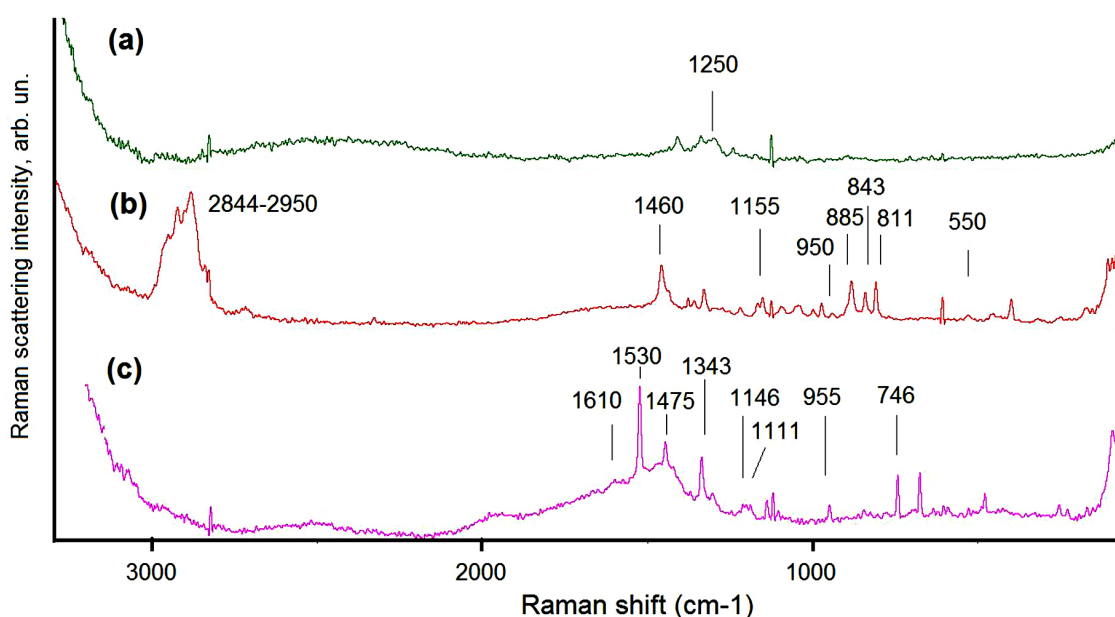


Fig. 5. Raman spectra of (a) AuNPs, (b) AuNP+MHDA, (c) AuNP+ MHDA+ChOX

to C = O and C-N, N-H bonds respectively. Some lines observed originate from amino acids consisting ChOX are more or less specific to the group of them. For example the band at 1457 cm<sup>-1</sup>, assigned to the vibrations of the CH group [31] is included also in the MHDA spectrum, as well as the sharp band at 1146 cm<sup>-1</sup> is associated with CCH and CCN bonds and is derived from few amino acids non-specifically [32]. The lines defined in the region of 500-1350 cm<sup>-1</sup> are more specific for a particular group of amino acids. For example, the band at 955 cm<sup>-1</sup> corresponds to arginine, the lines between 800 cm<sup>-1</sup> and 900 cm<sup>-1</sup> – to glycine as well as to alanine, whereas the line at 749 cm<sup>-1</sup> is attributed to tryptophan [33]. Some recorded lines derived from the FAD

prosthetic group (non-proteinaceous part of enzyme) and they are important information about enzyme structure. The line at 1111 cm<sup>-1</sup> could be assigned to the C = C bond vibration [33]. Further bands at about 1190 cm<sup>-1</sup> and 1230 cm<sup>-1</sup> correspond to the P-O symmetric and asymmetric vibrations, respectively [34]. The adenine band and ring I modes [35] are observed at 1343 cm<sup>-1</sup> and 1305 cm<sup>-1</sup> and they are derived from the same prosthetic group. Proposed identification of lines observed in the Raman spectra [17] are collated in Table 2.

It is well known [7,37] that when the size of nanoparticles is reduced, the lines amplitude is increased. If the amplitude of the line at 1530 cm<sup>-1</sup> can be used to measure the amplification

TABLE 2

Identification of the lines observed in the Raman spectra (Fig. 5)

	Position of line or group of lines (cm <sup>-1</sup> )	Sample	Identification	Reference
1	2844-2950	AuNP+MHDA	C-H stretch	27
2	1610	AuNP+MHDA+ChOX	C = O	29
3	1530	AuNP+MHDA+ChOX	N-H bend, C-N stretch, and N-C-O	29
4	1460 / 1457	AuNP+MHDA and AuNP+MHDA+ChOX	C-H bend (scissors)	30
5	1343 and 1305	AuNP+MHDA+ChOX	adenine amino acid and ring I of FAD	30, 34
6	1250	AuNP matrix	Plazmon, AuNP	27
7	1220	AuNP+MHDA+ChOX	C-N stretch and N-H bend	29
8	1190 and 1230	AuNP+MHDA+ChOX	P-O symmetric and asymmetric from FAD	34
9	1155	AuNP+MHDA	C-O stretch	28, 36
10	1146	AuNP+MHDA+ChOX	CCH and CCN	30
11	1111	AuNP+MHDA+ChOX	C = C from FAD	33
12	955	AuNP+MHDA+ChOX	arginineaminoacid	28
13	950	AuNP+MHDA	C-S stretch	36
14	800-900	AuNP+MHDA+ChOX	glycine and alanine amino acid	28
15	811, 843, 885	AuNP+MHDA	C-H wagging and out of plane	27, 36
16	749	AuNP+MHDA+ChOX	tryptophanaminoacid	32
17	550	AuNP+MHDA	C-C-O in plane deformation vibration	36

in the Raman signal due to AuNPs, this enhancing from 80 nm to 42 nm construct is in the ratio 10:350 (Fig. 5). We supposed that compared to the free enzyme the enhancing of the signal is about 3500 for 0,5 mg/ml of the enzyme concentration in colloidal solution [17].

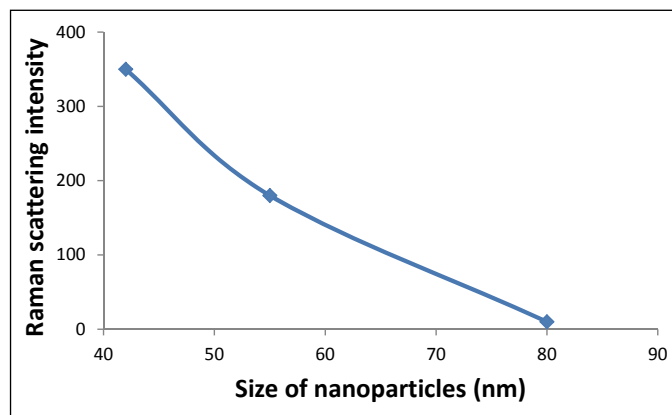


Fig. 6. Effect of nanoparticles size on the enhancing of the Raman scattering intensity

#### 4. Concluding remarks

Gold nanoparticles were synthesized by modified Turkevich method in three different sizes with diameter between 42 and 80 nm. The binding of ChOX via MHDA linker to the particles was confirmed by the protein concentration measurement as well as FTIR spectroscopy. Because of the unique properties of AuNPs, the nanoparticles were used as a matrix for construction the biological active biosensor element. The prepared construct is useful for cholesterol concentration control in two different ways: for bioelectrochemical and optical detection method. Bioactivity studies of the free and bound ChOX revealed that prepared construct is active (with the activity level 2,56 U/mg). As a result of the binding to the AuNPs, the storage stability of ChOX was considerably. The phenomenon of Surface Enhanced Raman scattering has been observed and used for the identification of functional groups existing in the enzyme and linkers. In current work, it is shown that besides typical functional groups of proteins (for example, N-H, C-N, N-C-O, CCN, and CNC bonds), the vibration lines attributed to the FAD prosthetic group indispensable for the activity of the enzyme have been observed (such as the PO and C = C binding). The next step will be observation the SERS line derived from cholesterol and observation in the real-time the chemical reaction for determined of the factor level. Simultaneously, the possibility of using the prepared bio-nanosystems for analytical purposes, namely, in the construction of biosensors is confirmed too.

#### REFERENCES

- [1] L. Barnes, A. Dereux, T.W. Ebbesen, *Nature* **424**, 824 (2003).
- [2] H. Zhang, D. Song, S. Gao, J. Zhang, H. Zhang, Y. Sun, *Sensor Actuat. B-Chem.* **188**, 548 (2013).
- [3] A.J. Haes, R.P. Van Duyne, *J. Am. Chem. Soc.* **124** (35), 10596 (2002).
- [4] J. Homola, S.S. Yee, G. Gauglitz, *Sensors and Actuat. B: Chem.* **25**, 3 (1999).
- [5] L. Rodriguez-Lorenzo, L. Fabris, R.A. Alvarez-Puebla, *Anal. Chim. Acta* **745**, 10 (2012).
- [6] S. Nie, S.R. Emory, *Science* **275**, 1102 (1997).
- [7] D.A. Stuart, J.M. Yuen, N. Shah, O. Lyandres, C.R. Yonzon, M.R. Glucksberg, J.T. Walsh, R.P. Van Duyne, *Anal. Chem.* **78** (20), 7211 (2006).
- [8] Y.H. Ngo, W.L. Then, W. Shen, G. Garnier, *J. Colloid. Interf. Sci.* **409**, 59 (2013).
- [9] U. Saxena, M. Chakraborty, P. Goswami, *Biosens. Bioelectron.* **26**, 3037 (2011).
- [10] N. Stasyuk, R. Serkiz, S. Mudry, G. Gayda, A. Zakalskiy, Y. Koval'chuk, M. Gonchar, M. Nisnevith, *Nanotechnology Development* 1, 11 (2011).
- [11] L. Pollegioni, L. Piubelli, G. Molla, *FEBS Journal* **23**, 1742 (2009).
- [12] A. Stępień, M. Gonchar, *ActaBiochim. Pol.* **60**, 401 (2013).
- [13] P. Srisawasdi, P. Jearanaikoon, N. Wetprasit, B. Sriwanthana, M.H. Kroll, P.H. Lolekha, *Clinica Chimica Acta* **372**, 103 (2006).
- [14] D.M. Yost, T.F. Anderson, *J. Chem. Phys.* **2**, 624 (1934).
- [15] J. Chermiti, M. Ben Ali, C. Dridi, M. Gonchar, N. Jaffrezic-Renault, Y. Korpan, *Sensor Actuat. B:Chem.* **188**, 824 (2013).
- [16] J. Kimling, M. Maier, B. Okenve, V. Kotaidis, H. Ballot, A. Plech, *J. Phys. Chem B* **110**, 15700 (2006).
- [17] R. Wojnarowska, J. Polit, D. Broda, M. Gonchar, E.M. Sheregii, *Applied Physics Letters* **106**, 103701 (2015).
- [18] A. Ravindran, A. Singh, A.M. Raichur, N. Chandrasekaran, A. Mukherjee, *Colloids and Surfaces B: Biointerfaces* **76**, 32 (2010).
- [19] J. Coates, *Interpretation of Infrared Spectra, A Practical Approach* in: R.A. Meyers (Ed.) *Encyclopedia of Analytical Chemistry* John Wiley & Sons Ltd, Chichester, 10815-10837 2000.
- [20] M. Yamamoto, Y. Sakurai, Y. Hosoi, H. Ishii, E. Ito, K. Kajikawa, Y. Ouchi, K. Seki, *Appl. Surf. Sci.* **427**, 388 (1999).
- [21] R.M. Hoth, *Self-assembly of Composite Semiconductor Nanomaterials: Applications in Patterning and Photoinduced Electron Transfer Processes*, Buffalo, 2006.
- [22] R.K. Gupta, M.P. Srinivasan, R. Dharmarajan, *Mater. Lett.* **67**, 315 (2012).
- [23] A. Barth, *Prog. Biophys. Mol. Bio.* **74**, 141 (2000).
- [24] A. Barth, *Biochim. Biophys. Acta* **1767**, 1073 (2007).
- [25] A.L. Morales-Cruz, R. Tremont, R. Martínez, R. Romanach, C.R. Cabrera, *Appl. Surf. Sci.* **241**, 371 (2005).
- [26] A. Barth, C.Q. Zscherp, *Rev. Biophys.* **35**, 369 (2002).
- [27] J. Mazur, B. Fanconi, *J. Chem. Phys.* **71**, 5069 (1979).
- [28] N.A. Atamas, A.M. Yaremko, T. Seeger, A. Leipertz, A. Bienko, Z. Latajka, H. Ratajczak, A.J. Barnes, *J. Mol. Struct.* **708**, 189 (2004).

- [29] J. Gelder, K. De Gussem, P. Vandenabeele, L. Moens, J. Raman Spectrosc. **38**, 1133 (2007).
- [30] R. Tuma, J. Raman Spectrosc. **36**, 307 (2005).
- [31] H. Shayani-Jam, D. Nematollahi, Chem. Commun. **46**, 409 (2010).
- [32] A. Brambilla, A. Philippidis, A. Nevin, D. Comelli, G. Valentini, D. Anglos, J. Mol. Struct. **1044**, 121 (2013).
- [33] A.L. Jenkins, R.A. Larsen, T.B. Williams, Spectrochim. Acta A **61**, 1585 (2005).
- [34] R.F. Brandao, R.L. Quirino, V.M. Mello, A.P. Tavares, A.C. Peres, F. Guinhos, J.C. Rubim, P.A.Z. Suarez, J. Braz. Chem. Soc. **20** (5), 954 (2009).
- [35] Y. Zheng, P.R. Carey, B.A. Palfey, J. Raman Spectrosc. **35**, 521 (2004).
- [36] G. Socrates, Infrared and Raman Characteristic Group Frequencies (John Wiley & Sons, 2004).
- [37] M.S. Anderson, Appl. Phys. Lett. **76**, 3130 (2000).

Received: 20 April 2015